Flexible, Wideband, Dual-band & Reconfigurable Direct-write Folded-Slot Antennas

Dimitris E. **Anagnostou**

South Dakota School of Mines and Technology, Electrical and Computer Engineering Department,
501 E. St. Joseph Str, Rapid City, South Dakota, 57701, USA. Email: danagn@ieee.org

Abstract

A design methodology that advances the capabilities of coplanar folded-slot dipole antennas (CFSA) is described. The methodology can transform single-band CFSAs by using symmetric and asymmetric radiation modes, to broadband, dual-band and reconfigurable (or tunable). This paper develops the theory for antenna operation, corrects an erroneous assumption that had been used since 1995 and presents design guidelines. A transmission-line model helps determine the tunable second resonance or bandwidth enhancement condition. Next, a reliable uni-planar reconfigurable CFSA without bias lines is developed and inkjet-printed on flexible Kapton®. Theoretical results are validated through measurements of prototypes developed recently at SDSMT.

1. Introduction

Coplanar folded-slot antennas (CFSAs) are of interest due to their typically large bandwidth (relative to other resonant planar antennas like dipoles), and their broadside radiation pattern that has higher gain than a dipole [1]. Recently, Anagnostou et al. showed that they consist of a folded-slot with an *outer* circumference of approximately one guided wavelength (λ_g). They are micromachinable, uniplanar, MMIC-compatible and can be direct-write printed on curved surfaces or thin layers over irregular holes. Efficient matching, bandwidth enhancement and dual-band techniques have been described. However, no unified design of broadband, dual-band and reconfigurable CFSAs exists.

Here, a unified design approach for dualband, wideband and/or reconfigurable CFSAs is presented. The design is based on analytical equations by using an offset feed (relative to the center of the folded slot) and by adjusting the length of the stubs inside the antenna aperture. The offset feed adds a second resonance f_2 without further modification or reconfiguration. The proposed method and graphs are simple to use and calculate accurately the antenna resonances. Design guidelines are shown for 2.4 – 5.25 GHz applications with various bandwidths. Next, a reconfigurable CFSA is achieved by placing metal strips and p-i-n diodes in critical places of the slot to manipulate the ground plane inner circumference. All designs are presented along with their theoretical, simulated and measured results that verified and validated the presented concepts. Since the length of the bias lines does not affect antenna performance, these antennas are advantageous. They are simple to design, feed and match while their fabrication is of low-cost. Whether by milling, direct-write printing or micromachining, they can be fabricated on practically any flexible or rigid substrate.

2. Wideband and Dual-band CFS Antennas

A reference center-fed CFSA (Fig. 1a) resonates at f_1=2.4 GHz and is designed and matched with standard techniques [1, 2], but by making its *outer* slot circumference (instead of the *mean*) equal to one wavelength λ_g [3]. An asymmetric off-center-fed CFSA is shown in Fig. 1b [4]. It consists of two open-circuited transmission line sections of different length and its equivalent circuit is shown in Fig. 1c. We will specify its second resonance f_2 by applying the transverse resonance technique [5] along its *x*-axis (Fig. 1b) at the terminals of the slot, at the T-junction where the 50-Ω CPW feedline separates into the two open-circuit stubs. This technique has been applied before with great accuracy in planar and conformal slots. Each stub presents a pure reactance, and the transverse resonant technique [5] states:

$$Z_L(x') + Z_R(x') = 0 \qquad (1)$$

where Z_L and Z_R are the input impedances to the left and right of the slot terminals (reference point). Since at f_1 most current flows around the slot, f_1 depends mostly upon the *outer* circumference of the slot and not so much on the *mean* circumference as mentioned in [1]. Also, f_1 is not affected by S or by the total stub length L_s. To estimate f_2, we use transmission line theory for the open-circuited sections and express (1) as:

$$jZ_0 \cot[\beta(\omega)d] + jZ_0 \cot[\beta(\omega)(L_s - d)] = 0 \quad \Rightarrow \quad \tan[\beta(\omega)L_s - \beta(\omega)d] = -\tan[\beta(\omega)d] \qquad (3)$$

978-1-4244-5118-0/11/$26.00 ©2011 IEEE

where $\beta(\omega)$ is the propagation constant of the line and d is in Fig. 1. Equation (3) holds when $\beta(\omega)L_s=n\pi$, n=1, 2,…N, or

$$L_s = \frac{n\lambda_g}{2} \qquad , n = 1,2,3.....N \tag{4}$$

where the CPW line λ_g is at f_2. For n = 1, (4) says that in addition to f_1, an off-centered fed CFSA will resonate also at a second frequency f_2 when $L_s = \lambda_g/2$ at that frequency. If f_2 is near f_1, a broadband mode is achieved, while if f_2 is far from f_1, a dual-band mode is obtained. Three prototypes were designed by offsetting the feedline of the 2.4 GHz reference CFSA by S. According to (4), L_s (and optionally L_f) were made $\lambda_g/2$ at each f_2. All dimensions are in Table I. The simulated $|S_{11}|$ (Fig. 2a) shows excellent agreement between calculated from (4), simulated (IE3D™) and measured f_2, as well as f_1 values. It also verifies that f_1 is independent of L_s and validates the use of *outer* circumference for it. Table II shows that (4) yields < 2% deviation from the calculated and simulated f_2.

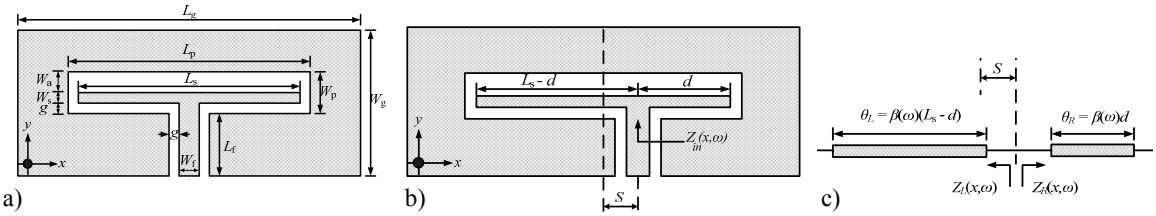

Fig. 1. Schematics of the CFSA: a) traditional center-fed, b) asymmetric, and c) transmission line model for (b).

The CFSA radiation mechanism differs for f_1 and f_2. At f_1 the antenna forms a resonant aperture, while at f_2 the stub resonates in a way similar to an offset-fed $\lambda/2$ dipole and so its Z_{in} depends upon its current distribution and is a function of the feed position (offset) S. This is shown in Fig. 2b where as a S/L_s increases, the matching of f_2 improves. *First*, in the wideband case (Fig. 2b) where f_1 = 2.4GHz and f_2 = 3 GHz, f_2 couples with the nearby f_1 resulting in a small drift (4%) from 2.4 to 2.5 GHz due to overcoupling. At S/L_s = 0.07, which means that S is equal to 0.07 of $\lambda_g/2$ at f_2, the two resonances are well-matched and broadband operation (~30% bandwidth) is obtained. This mode persists until S/L_s=0.16, and vanishes thereafter. Note, for $S/L_s \le 0.06$, the bandwidth (shown vs. S/L_s in Fig. 2c) is the sum of the two bands. *Second*, a dual-band WLAN CFSA at 2.4 and 5.25GHz was studied. Fig. 2b shows no broadband mode when f_2 is far from f_1. However the Smith Charts (Fig. 3a) prove that the S/L_s ratio affects the matching and bandwidth at f_2 (as expected) but not at f_1. This tunability of f_2 with S/L_s, allows the antenna to be matched at both resonances and also with impedances other than 50Ω (e.g. 25, 75, 100, etc) by offsetting the feed. Of course the matching at a different impedance should be done also for f_1. The bandwidth of f_2 vs. S/L_s for dual-band antennas is in Fig. 3b. Good $|S_{11}|$ and bandwidth at f_2 were obtained for $0.04 \le S/L_s \le 0.09$. The design of broadband and dual-band CFSAs is summarized:

1) Design and match a single-band, CFSA at the lower f_1, according to [1, 2] but with *outer* slot circumference λ_g at f_1.
2) Make the length of the stub located inside the slot equal to half-wavelength ($\lambda_g/2$) at f_2 as given from (4).
3) Make the length of the 50-Ω CPW feeding line equal to half a wavelength ($\lambda_g/2$) at f_2.
4) Select an appropriate feed offset S from Fig. 2c for the broadband mode or from Fig. 3b for the dual-band mode.
5) If needed, adjust the dimension W_a to match better the antenna.

This methodology is now applied to design the broadband and dual-band CFSAs that are shown along with their measurements in Fig. 4a-b. A 32 mil RO4003C substrate is used. An ε_{r_eff}=1.76 can be calculated and the perimeter is $P=2(W_p+W_a)=\lambda_g$=94mm. This step is important and differs from the widely-used mean slot perimeter [1]. An offset S/L_s=0.07 is used from Fig. 2c. Measurements show two resonances at 2.55 and 3.1 GHz (29.6% bandwidth), with <2% shift from simulations, and 6% shift from the 2.4 GHz due to overcoupling. Measured and simulated patterns (Fig. 4c) at 2.5 GHz, are symmetric (only half plane shown) and typical for CFSAs: i.e. near omni-directional H-plane, and ∞-shaped E-plane. The maximum measured gain is 4.8 dBi (2.5 GHz) and 3.5dBi (3.1 GHz), significantly higher than $\lambda_g/2$ dipoles. For CFSAs, the co-pol in the H-plane is E_φ and in the E-plane is E_θ. The cross-pol patterns (E_θ in H-plane, and E_φ in E-plane) are strong at 3.1 GHz since they are the major radiating fields at f_2. This is comprehended by reviewing the current at 2.5 GHz and 3.1 GHz in Fig. 4d. At 2.5 GHz (Fig. 4d-i), the current is large around the outer circumference of the slot that resonates and the current on the stub arms flows in opposite directions. At 3.1 GHz though, most current is on the stub and nearby ground, and along the stub it flows in the same direction as in a $\lambda_g/2$ dipole and thus enhancing cross-pol at f_2. So, radiation at 2.5 GHz originates from magnetic conducting surfaces while at 3.1 GHz from electric, and is perpendicular polarized as explained by Booker's extension of Babinet's principle onto antennas that accounts for polarization. The same also happens with the dual-band CFSA patterns (not shown for

brevity), and with most (if not all) offset CFSAs, indicating that each band's radiating mechanism is decoupled. A dual-band antenna at 2.4 and 5.25 GHz was also designed by with the same steps by selecting S/L_s=0.08 from Fig. 3b. Measurements in Fig. 4b show < 3% shift from simulations. More results and patterns will be presented. Table III has a summary of all broadband and dual-band CFSA results.

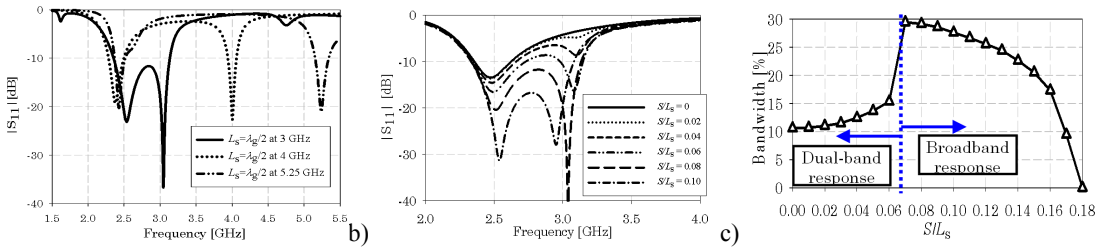

Fig. 2. a) Simulated $|S_{11}|$ of broadband (3 GHz) and dual-band (4 and 5.25 GHz) CFSAs. b) Simulated $|S_{11}|$ of broadband 2.4–3 GHz CFSA for different S/L_s ratios of feed offset to stub length. c) bandwidth vs. S/L_s for the 2.4-3 GHz CFSA. The dual-band bandwidth is the sum of the two bands that combine and form the broadband CFSA at $S/L_s \sim 0.07$.

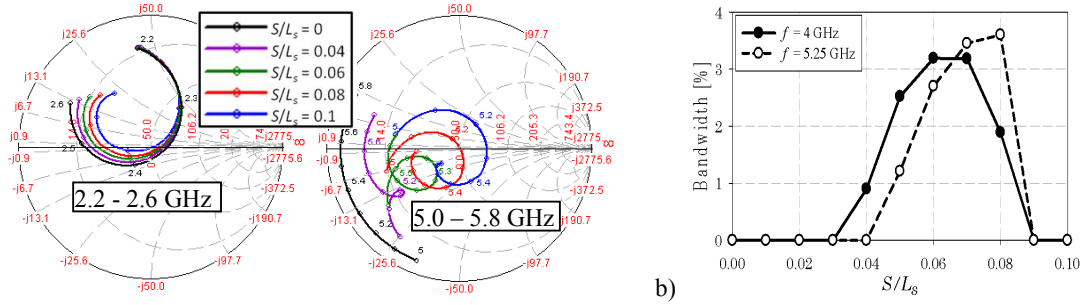

Fig. 3. a) Impedance matching of the 2.4 and 5.25 GHz dual-band CFSA for various feed offsets. The input impedance of the 2.4 GHz resonance remains constant for all S/L_s ratios, while at 5.25 GHz it increases rapidly with S/L_s. b) Simulated bandwidth of the second band only vs. S/L_s. The maximum bandwidth is typically obtained around S/L_s~0.07.

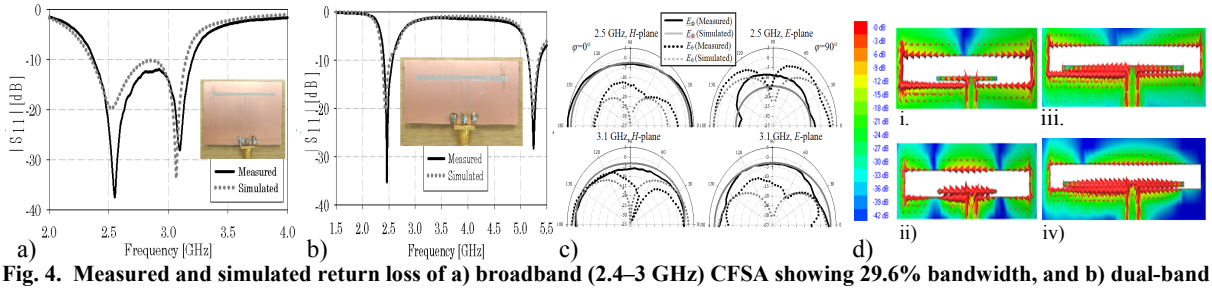

Fig. 4. Measured and simulated return loss of a) broadband (2.4–3 GHz) CFSA showing 29.6% bandwidth, and b) dual-band (2.4 and 5.25 GHz) CFSA with f_2/f_1=2.18. Insets show the fabricated prototypes. c) Measured and simulated patterns of broadband CFSA. d) Currents at i-ii) 2.4 & 5.25 GHz (dual-band), and iii-iv) 2.5 & 3.1 GHz (broadband).

3. Reconfigurable and Direct-Write Printed CFSA

Using the above methodology and the Fig. 1a schematic, the first fully functional direct-write printed reconfigurable antenna was designed and fabricated. A symmetric feed is chosen as 2.7 and 3.7 GHz suffice to prove the concept. Metal strips inside the aperture are attached to the ground with p-i-n diodes that effectively connect or disconnect them to the ground, changing the perimeter of the slot when conducting, and thus changing the resonant frequency of the antenna. When connected, the strips become part of the ground and the slot perimeter is reduced and resonates at f_{on} = 3.7 GHz. In contrast, the slot perimeter is extended when the diodes are unbiased, forcing the antenna to resonate at f_{off} = 2.7 GHz. When diodes are 'off', their DC bias lines are separated from the antenna RF and ground parts, and so they do not shift the f_{off}. Also, when diodes are 'on', the lines become part of the antenna ground and simply increase its size. So, their effect on f_{on} is negligible and thus CFSAs do not require DC bias circuitry to nullify the effect of bias lines, which can then be made with any length. The antenna was direct-write printed on a very flexible 100 μm thick Kapton® substrate. Printing was made with photoconductive nano-inks at 40°C using the M^{3}D maskless mesoscale material deposition system. A photo of a flexed and fully functional prototype and its measured $|S_{11}|$ is in Fig.

5. It shows < 2.1% shift from simulations. Patterns were measured at both states and the measured gain was 3.61 dBi at 2.7 GHz (off) and 4.04 dBi at 3.7 GHz (on). Patterns at both frequencies were similar as expected.

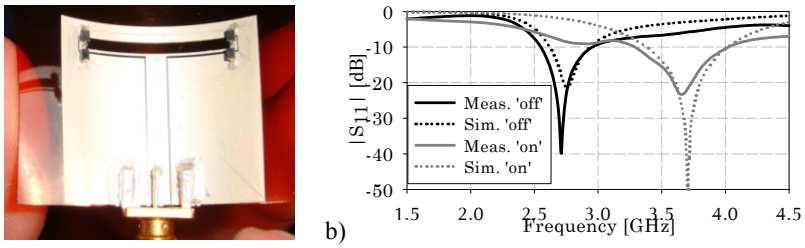

Fig. 5. a) Photo of the first direct-write printed reconfigurable CFSA, and b) its $|S_{11}|$ response at both configurations.

4. Conclusions

A design methodology that enhances the performance and transforms single-band CFSAs to wideband, dual-band and reconfigurable CFSAs was introduced. Bandwidth up to ~30%, and a dual-band frequency ratio limited by the third harmonic of f_1 (i.e. $f_2/f_1 < 3$) can be obtained. The advantages of the reconfigurable design are that it does not require a DC bias circuit and its bias lines can be of any length, which make the fabrication of it an extremely low-cost procedure. This was the first reconfigurable antenna to be direct-write printed. It was fabricated on flexible Kapton® with conductive nano-inks using M^3D. All fabricated CFSAs exhibited excellent performance as predicted by the calculations and simulations. The design method is scalable to other frequency ratios and impedances.

TABLE I
DIMENSIONS OF BROADBAND AND DUAL-BAND CFSAS [IN MM].

Parameter	f_2 = 3 GHz	f_2 = 4 GHz	f_2 = 5.25 GHz
L_g	55	55	55
W_g	44.3	37.8	30
L_p	44.5	44.5	44.5
W_p	2.06	2.36	2.5
L_s	35.6	27.1	20.4
W_s	0.35	0.35	0.35
W_a	1.5	1.8	1.8
W_f	3.1	3.1	3.1
g	0.21	0.21	0.21
L_f	35.6	27.1	20.4
S	2.14	1.62	1.63

f_1 for all designs is 2.4 GHz

TABLE II
CALCULATED AND SIMULATED F_2 FOR OFF-CENTER-FED CFSA.

Calculated from (4)	Simulated (IE3D)	|Deviation|
3 GHz	3.05 GHz	1.67 %
4 GHz	4.01 GHz	0.25 %
5.25 GHz	5.26 GHz	0.19 %

TABLE III.
RESONANT FREQUENCIES AND BANDWIDTH FOR CFSAS

Design	Measured (Simulated)			
	f_1 [GHz]	f_2 [GHz]	f_1 BW [%]	f_2 BW [%]
Broadband	2.55 (2.51)	3.09 (3.06)	[---- 29.7 (27.8) ----]	
Dual-Band	2.47 (2.4)	5.25 (5.26)	6.2 (5.7)	4.1 (3.6)

5. Acknowledgments

Work supported by DOD #W911NF-09-1-0277, NSF #0824034 and #0903804 and NASA #NNX07AL04A.

6. References

[1] T. M. Weller, L. P. B. Katehi and G. M. Rebeiz, "Single and double folded-slot antennas on semi-infinite substrates", *IEEE Trans. on Antennas and Propagation*, v.43, i.12, pp. 1423-1428, Dec. 1995.

[2] N. Lopez-Rivera, and R. A. Rodriguez-Solis, "Impedance matching technique for microwave folded slot antennas," *Antennas and Propagation Society International Symposium, 2002. IEEE*, v. 3, 2002, pp. 450 – 453.

[3] D. E. Anagnostou and A. A. Gheethan, "A coplanar reconfigurable folded slot antenna without bias network for WLAN applications", *Antennas and Wireless Propagation Letters*, vol. 8, 2009, pp. 1057-1060.

[4] A. A. Gheethan and D. E. Anagnostou, "Broadband and Dual-Band Coplanar Folded-Slot Antennas (CFSAs)", *IEEE Antennas and Wireless Propagation Magazine* (in press)

[5] C. Balanis, Advanced Engineering Electromagnetics, *Wiley*, 1989, Ch. 8, pp. 410-413.